Cancer Cell
Article

Cell PRESS

B55β-Associated PP2A Complex Controls PDK1-Directed Myc Signaling and Modulates Rapamycin Sensitivity in Colorectal Cancer

Jing Tan,[1,2] Puay Leng Lee,[1] Zhimei Li,[1] Xia Jiang,[1] Yaw Chyn Lim,[2] Shing Chuan Hooi,[2] and Qiang Yu[1,2,3,*]
[1]Cancer Biology and Pharmacology, Genome Institute of Singapore, Agency for Science, Technology and Research, Biopolis, Singapore
[2]Department of Physiology, Yong Loo Lin School of Medicine, National University of Singapore, Singapore
[3]Cancer and Stem Cell Biology, DUKE-NUS Graduate Medical School of Singapore, Singapore
*Correspondence: yuq@gis.a-star.edu.sg
DOI 10.1016/j.ccr.2010.10.021

SUMMARY

The PP2A serine/threonine protein phosphatase serves as a critical cellular regulator of cell growth, proliferation, and survival. However, how this pathway is altered in human cancer to confer growth advantage is largely unknown. Here, we show that *PPP2R2B*, encoding the B55β regulatory subunit of the PP2A complex, is epigenetically inactivated by DNA hypermethylation in colorectal cancer. B55β-associated PP2A interacts with PDK1 and modulates its activity toward Myc phosphorylation. On loss of *PPP2R2B*, mTORC1 inhibitor rapamycin triggers a compensatory Myc phosphorylation in PDK1-dependent, but PI3K and AKT-independent manner, resulting in resistance. Reexpression of *PPP2R2B*, genetic ablation of PDK1 or pharmacologic inhibition of PDK1 abrogates the rapamycin-induced Myc phosphorylation, leading to rapamycin sensitization. Thus, PP2A-B55β antagonizes PDK1-Myc signaling and modulates rapamycin sensitivity.

INTRODUCTION

Protein phosphatase 2A (PP2A) functions as a multimetric enzyme that contains the catalytic C subunit, a scaffolding A-subunit and one of a large array of regulatory B-subunits. Eukaryotic cells contain over 200 biochemical distinct PP2A complexes derived from differential combinations of A, B, C, and other subunits. The regulatory subunits are expressed in a tissue-specific manner, leading to the presence of different PP2A complexes in different mammalian tissues (Virshup and Shenolikar, 2009). Moreover, it is these regulators, rather than the catalytic subunit, that provides the substrate specificity and catalyzes distinct dephosphorylation events that result in specific functional outcomes.

Although a tumor suppressor role of PP2A has been previously shown in a variety of immortalized human cell types (Chen et al., 2004; Eichhorn et al., 2009; Janssens and Goris, 2001; Rangarajan et al., 2004; Sablina et al., 2007; Zhao et al., 2003), the genetic and/or the epigenetic evidence pointing to a prevalent inactivation of PP2A in human malignancy have not been reported. Somatic mutations in the A subunit of the PP2A complex, which can result in the loss of B subunit binding (Ruediger et al., 2001), were found in only up to 15% of some human cancers (Calin et al., 2000; Ruediger et al., 2001; Takagi et al., 2000; Tamaki et al., 2004; Wang et al., 1998; Westermarck and Hahn, 2008), and the reduced expression of PP2A subunit B56γ has been reported only in some cancer cell lines (Chen et al., 2004; Zhao et al., 2003). In general, the genetic or epigenetic changes of PP2A complexes in human cancer remains to be defined, as is its impact on cancer signaling and therapeutic responses to targeted therapy.

One of the PP2A regulated cancer signaling pathways is the mTOR pathway, a key component of PI3K pathway that many cancer cells are "addicted" to for growth advantage (Guertin and Sabatini, 2007; Sabatini, 2006). Although small molecule mTORC1 inhibitors, such as rapamycin and its analogs have

Significance

Clinical evidence pointing to a wide occurrence of PP2A tumor suppressor inactivation has not been previously provided. Here, we show the occurrence of epigenetic silencing of PP2A regulatory B55β subunit, encoded by *PPP2R2B*, in > 90% human colorectal cancer. Loss of *PPP2R2B* results in PDK1-dependent, but PI3K-independnt induction of Myc phosphorylation in response to mTOR inhibitor rapamycin, resulting in rapamycin resistance. Restoration of *PPP2R2B* or inhibition of PDK1 abrogates rapamycin-induced Myc phosphorylation, resensitizing rapamycin. Our data demonstrate an alternate mechanism underlying rapamycin resistance, which is independent of PI3K-AKT. Thus, *PPP2R2B* is likely to be a useful biomarker to predict rapamycin sensitivity. Further, we show that a combination of PDK1 inhibitor with rapamycin might provide a treatment strategy for colorectal cancer.
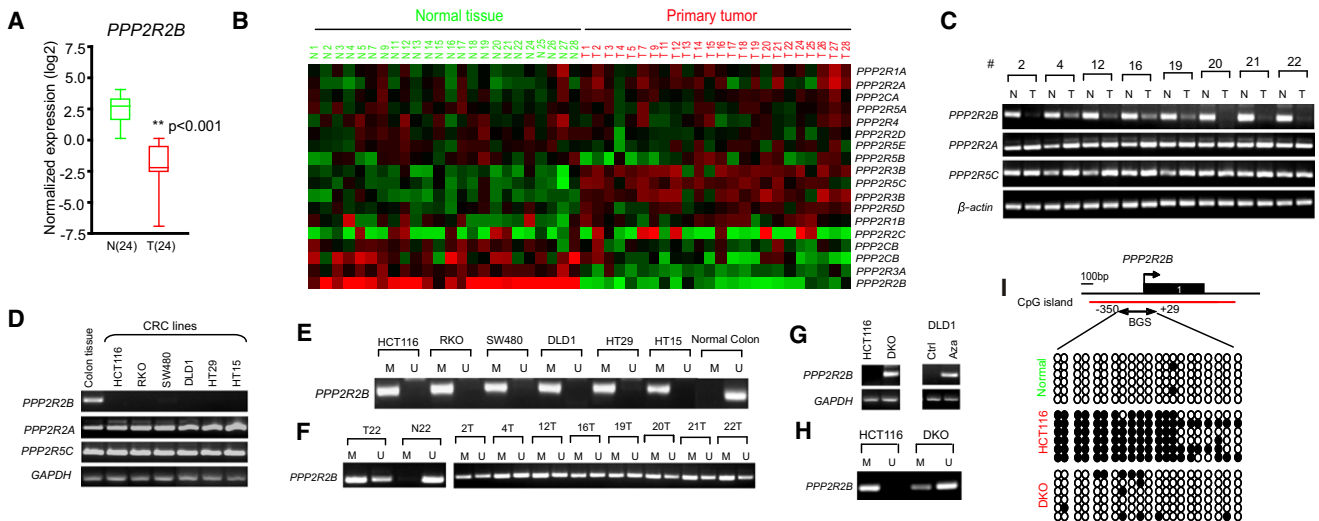
Figure 1. Loss of *PPP2R2B* Expression by Promoter DNA Hypermethylation in CRC

(A) Box-plot showing the differential expression of *PPP2R2B* mRNA levels in 24 pairs of patient-derived CRC and matched normal colon mucosa as determined by Illumina array analysis. P value for difference between tumor and normal is indicated.

(B) Hierarchical clustering of expression levels of PP2A subunits in 24 pairs of colorectal tumors (T) and matched normal mucosa (N).

(C) RT-PCR analysis of *PPP2R2B*, *PPP2R2A*, and *PPP2R5C* expression from eight randomly selected pairs of human CRC (T) and matched mucosa (N).

(D) RT-PCR analysis of *PPP2R2B*, *PPP2R2A*, and *PPP2R5C* in a panel of CRC cell lines compared to the normal colon tissue as well as nontransformed cell lines.

(E) Methylation specific PCR (MSP) analysis of *PPP2R2B* promoter in CRC cell lines and nontransformed cells. M: methylated; U: unmethylated.

(F) MSP analysis of *PPP2R2B* promoter in eight tumor and normal controls. M: methylated; U: unmethylated.

(G) RT-PCR analysis of *PPP2R2B* in HCT116 and DKO or DLD1 cells treated with or without 5-AzaC (5 μM) for 3 days.

(H) MSP analysis of *PPP2R2B* promoter in HCT116 and DKO cells. M: methylated; U: unmethylated.

(I) Methylation analysis of *PPP2R2B* promoter by bisulfite-sequencing analysis (BGS). The region analyzed is indicated. The arrow indicates the transcriptional start site. Open circles represent unmethylated CpGs; closed circles denote methylated CpGs. See also Figure S1 and Tables S1 and S2.

shown promise as cancer therapeutics and have been approved for clinical application (Guertin and Sabatini, 2007; Hudes et al., 2007), they have had only limited successes and clinical outcomes are mostly unpredictable. Although a known mechanism of rapamycin resistance is linked to its feedback activation of AKT phosphorylation through PI3K and mTORC2 (O'Reilly et al., 2006; Sarbassov et al., 2006), a deeper understanding of the resistance mechanisms and the identification of biomarkers that help predict therapeutic responses have become important topics (Mao et al., 2008; Scott et al., 2009; Thomas et al., 2006).

RESULTS

Loss of *PPP2R2B* Expression by DNA Hypermethylation in Colorectal Cancer

Given the low frequency of mutations found in PP2A family members in human malignancy, including colorectal cancer (CRC), we sought to determine whether they are epigenetically inactivated in CRC. Through interrogating expression data of a series of CRC cell lines we published previously (Jiang et al., 2008), we found that *PPP2R2B*, encoding B55β, is the only subunit that is consistently downregulated or silenced in all examined CRC cell lines, but not in the normal colon mucosa samples (see Table S1 available online). The significant downregulation of *PPP2R2B* was further validated using gene expression array data of 24 pairs of patient-derived CRC tumors and matched normal mucosa controls (p < 0.01) (Figure 1A), and

this appeared to occur in >90% of CRC samples (Figure 1B; Table S2). Semiquantitative and quantitative RT-PCR analysis confirmed the *PPP2R2B* downregulation in eight randomly selected CRC compared to the matched controls, as well as in a series of CRC cells lines (Figures 1C and 1D; Figure S1A), but not in the nontransformed epithelial cells (Figure S1B). By contrast, *PPP2R2A* (B55α) and *PPP2R5C* (B56γ), which has been previously reported to be downregulated in lung cancer (Chen et al., 2004), were not downregulated in CRC (Figures 1C and 1D).

We next determined whether the loss of *PPP2R2B* expression in CRC is associated with promoter DNA hypermethylation. Methylation-specific PCR (MSP) analysis revealed a hypermethylated *PPP2R2B* promoter in CRC cell lines, as well as in all eight CRC tumor samples examined, but not in their matched normal controls (Figures 1E and 1F), nor in nontransformed epithelial cells (Figure S1C). Furthermore, HCT116 cells deleted of both *DNMT1* and *DNMT3B* (DKO) or DLD1 cells treated with 5-aza-dC reexpressed *PPP2R2B* (Figure 1G), correlated with a demethylated *PPP2R2B* promoter in DKO, as demonstrated by both MSP and bisulfate genomic sequencing (Figures 1H and 1I). Taken together, these results demonstrate that *PPP2R2B* is epigenetically silenced in CRC through promoter DNA hypermethylation. Moreover, Oncomine data mining reveals that *PPP2R2B* is also significantly downregulated in other human cancers, such as bladder, brain and esophagus carcinomas (Figure S1D).
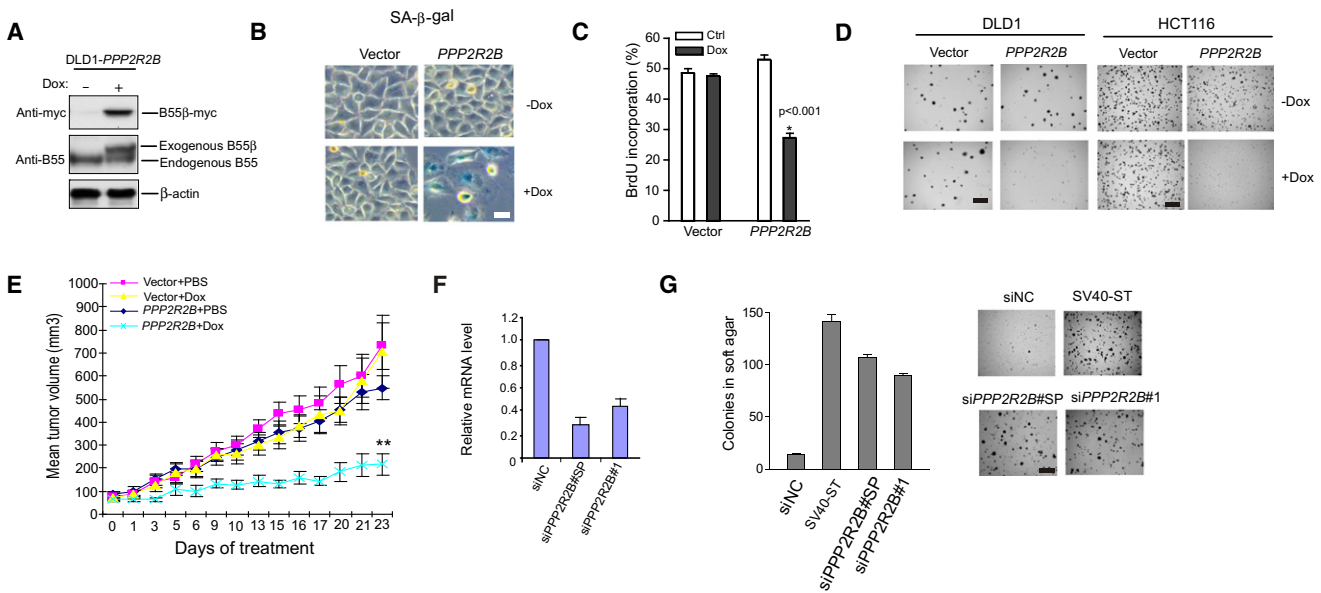
Figure 2. Gain- or Loss-of-Function Analysis of *PPP2R2B*

(A) Immunoblot analysis of DLD1-*PPP2R2B* cells on exogenous B55β and endogenous B55 using anti-Myc tag or anti-B55 subunit antibody. Cells were treated with or without 10 ng /ml doxycycline (Dox) for 3 days.

(B) SA-β-gal assay of DLD1-*PPP2R2B* or vector control cells treated with or without Dox for 96 hr. Scale bars, 100 μm.

(C) BrdU incorporation of DLD1-*PPP2R2B* or vector control cells treated with or without Dox for 96 hr. Shown is mean ± SD of three independent experiments. **p < 0.001.

(D) Anchorage-independent growth assessed by soft agar assay in DLD1-*PPP2R2B* or HCT116-*PPP2R2B* cells, treated with or without Dox for 12 days. Scale bar, 10 μm.

(E) Xenograft tumor growth of DLD1-*PPP2R2B* or control cells in nude mice treated with Dox at 100 mg/kg daily as described in Experimental Procedures. Error bars represent mean ± SD (n = 8 per group). **p < 0.01 (independent t test).

(F and G) HEK-TERV cells were transfected with a *PPP2R2B* smart pool siRNA (SP) or an independent *PPP2R2B* siRNA and the *PPP2R2B* mRNA was assessed by TaqMan assay (F) and the colony formation capacity was assessed by soft-agar assay (G). Shown on the left is quantification of number of colonies after 14 days from three independent experiments. The representative images of three independent experiments are shown on the right. SV40 small antigen (ST) expressing HEK-TERV cells were used as positive control. Scale bar, 10 μm. Error bar shows mean ± SD of triplicates. See also Figure S2.

PPP2R2B Re-Expression in CRC Cells Results in Senescence, Decreased Cell Proliferation, and Xenograft Tumor Growth Inhibition

Loss of *PPP2R2B* expression in cancer suggests it normally may function to inhibit cancer proliferation. To investigate this possibility, we established stable DLD1 and HCT116 cell lines with doxycycline (Dox) inducible expression of a Myc-tagged *PPP2R2B*, designated as DLD1-*PPP2R2B* or HCT116-*PPP2R2B*. As shown in DLD1-*PPP2R2B* cells, addition of Dox resulted in PPP2R2B-Myc (B55β-Myc) expression at levels comparable to the endogenous expression of other three B55 subunits that are not silenced in DLD1 cells, as detected using an antibody recognizing total four B55 subunits (α, β, γ, and σ) (Figure 2A). To further demonstrate that exogenous B55β (PPP2R2B) was expressed in a level that is close to a physiologically relevant level, we compared the exogenous B55β with normal tissues or other cancer cell lines that express abundant endogenous B55β by both RT-PCR and western blot analyses (Figures S2A and S2B). The results show that B55β-Myc is induced in CRC cells at a level that is near the physiological range. Under this condition, restored expression of B55β resulted in a typical senescence phenotype, including enlarged and flattened cell morphology, as well as increased senescence-associated β-galactosidase (SA-β-Gal) in a time-depen-

dent manner (Figure 2B; Figure S2C). Accordingly, DNA synthesis as measured by BrdU incorporation decreased markedly after *PPP2R2B* expression by Dox (Figure 2C), indicative of inhibition of cell proliferation. Furthermore, *PPP2R2B* restoration caused a strong inhibition of anchorage-independent growth in soft agar (Figure 2D). The strong growth inhibitory effect of B55β was further confirmed in two additional CRC cell lines by using retroviral transduction of both GFP and B55β, which resulted in similar morphological changes (Figure S2D) and inhibition of growth in soft agar (Figure S2E).

To assess the capacity of B55β in tumor growth inhibition in vivo, Dox-inducible DLD1 cells expressing B55β or the empty vector were subcutaneously injected into nude mice and tumor growth was monitored for 3 weeks with or without daily Dox treatment. The data showed that the tumor growth derived from DLD1-*PPP2R2B* cells was markedly inhibited in mice treated with Dox, whereas the tumor growth from the DLD1 cells expressing the control vector was unaffected by Dox treatment (Figure 2E). This result confirmed the growth inhibitory activity of B55β in a xenograft mouse model.

PPP2R2B Knockdown Promotes Cell Transformation

We next addressed whether ablation of *PPP2R2B* is sufficient to promote cell transformation in immortalized human embryonic
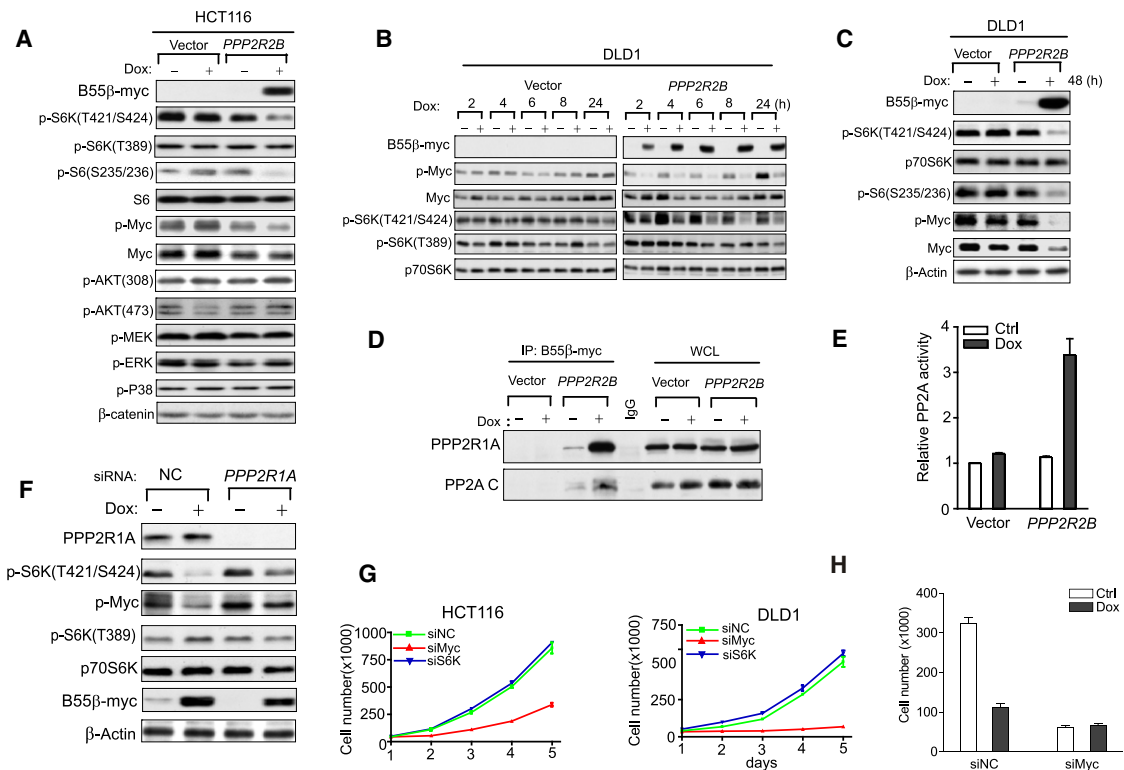
Figure 3. Restoration of *PPP2R2B*-PP2A Complex Results in Inhibition of p70S6K and Myc Phosphorylation

(A) Immunoblot analysis of HCT116-*PPP2R2B* or the vector control cells for indicated proteins in the presence or absence of Dox for 48 hr.

(B and C) Immunoblot analysis of DLD1-*PPP2R2B* or the vector control cells treated with or without Dox for the indicated length of times.

(D) Coimmunoprecipitation of PP2A scaffolding A subunit and catalytic C subunit with *PPP2R2B*. DLD1-*PPP2R2B* or vector control cells were treated with Dox and *PPP2R2B* was immunoprecipitated with anti-Myc tag antibody. WCL, whole cell lysates.

(E) Serine/threonine phosphatase activity for DLD1-*PPP2R2B* or vector control cells. Protein phosphatase activity of the immunoprecipitates of *PPP2R2B*-Myc was measured in triplicates from three independent experiments.

(F) Immunoblot analysis of DLD1-*PPP2R2B* cells for Myc, p-Myc (S62), and p70S6K, treated *PPP2R1A* siRNA or a negative control siRNA, with or without Dox treatment.

(G) Growth curve of HCT116 and DLD1 cells treated with Myc, p70S6K siRNA, or negative control siRNA for indicated days.

(H) Growth inhibition of DLD1 cells induced by Myc knockdown, *PPP2R2B* expression or both. Data in (E), (G), and (H) represent mean ± SD of triplicates or three independent experiments. See also Figure S3.

kidney (HEK) fibroblasts expressing hTERT and oncogenic Ras (HEK-TERV). In this previously well-characterized transformation model, inhibition of PP2A by overexpression of small T antigen results in efficient transformation (Chen et al., 2004; Hahn et al., 2002; Sontag et al., 1993). Small interfering RNA (siRNA)-directed knockdown by targeting two different regions of *PPP2R2B* mRNA also resulted in an enormous increase in anchorage-independent growth of HEK-TERV cells (Figure 2F &G). A similar result was also obtained in HEK-TERV cells expressing a stable shRNA targeting *PPP2R2B* (Figure S2F). On the basis of both the gain- and loss-of-function data, we propose that loss of *PPP2R2B* facilitates oncogenic transformation.

PPP2R2B-Associated PP2A Complex Modulates Phosphorylation of Myc and p70S6K in CRC Cells

The PP2A B regulatory subunits confer substrate specificity for dephosphorylation events in a cell- and context-dependent manner (Virshup and Shenolikar, 2009). Several oncogenic proteins, including AKT, p70S6K, mTOR, β-catenin, and Myc,

have been previously identified to be the substrates of PP2A in various cell systems (Andrabi et al., 2007; Arnold and Sears, 2008; Peterson et al., 1999; Seeling et al., 1999; Yeh et al., 2004). To dissect out the possible mechanisms responsible for the growth inhibitory effect of B55β, we began with the HCT116-*PPP2R2B* cells to probe several oncogenic signaling pathways known to be important in CRC that might be affected by PP2A (Figure 3A). The analysis led to the identification of two phosphorylation events that are inhibited by *PPP2R2B* reexpression after Dox treatment. First, using phosphorylation specific antibodies, we show that the phosphorylation of p70S6K at T421/S424 was markedly reduced on *PPP2R2B* re-expression, whereas the phosphorylation at T389 appeared to be unaffected, suggesting a site-specific modulation of p70S6K by *PPP2R2B*. Second, c-Myc phosphorylation, detected by using a phospho-Myc antibody specific for S62, was also downregulated on *PPP2R2B* reexpression. Other oncogenic signals, such as p-AKT, p-ERK, β-catenin, and p-p38 were not noticeably affected by *PPP2R2B* re-expression (Figure 3A).

The effects of B55β on p70S6K and c-Myc (thereafter referred to as Myc) were further confirmed in DLD1 cells in a time-course analysis (Figure 3B). The data showed that Dox induction of *PPP2R2B* expression resulted in a rapid dephosphorylation of Myc and p70S6K (T421/S424, but not T389) relative to total p70S6K and Myc protein levels, suggesting that these changes are the early effects of B55β and unlikely to be the secondary effect of growth inhibition. The decreased Myc phosphorylation eventually resulted in less protein accumulation by 48 hr of Dox treatment (Figure 3C), which is consistent with the previous finding that increased Myc phosphorylation at S62 correlates with Myc protein accumulation (Arnold and Sears, 2006; Junttila et al., 2007; Yeh et al., 2004). Thus, p70S6K and Myc are two downstream signals affected by B55β-PP2A complex, whereas no marked differences were observed in the expression levels nor phosphorylation status of other oncogenic signaling pathways known to be important in colorectal cancer.

Of note, *PPP2R2B* re-expression had no effect on AKT T308 phosphorylation, which is known to be targeted by PP2A/B55α or B56β complex in NIH 3T3 cells (Kuo et al., 2008; Padmanabhan et al., 2009), neither on β-catenin phosphorylation that is a target of PP2Aα in CRC (Su et al., 2008). In addition, in human mammary epithelial cell cells, SV40 small t antigen(ST)-mediated PP2A inhibition is associated with increased AKT S473 phosphorylation and the mTOR-mediated p70S6K T389 phosphorylation (Andrabi et al., 2007; Chen et al., 2005; Zhao et al., 2003), but these changes were not observed here, in this cellular context. These findings are consistent with the substrate specific functions of different PP2A/B subunits in tissue specific contexts and show that B55β-associated *PP2A* complex is distinguished from the other PP2A complexes by affecting different downstream substrates.

To demonstrate that ectopic B55β in fact interacts with other PP2A subunits to form an active PP2A complex, we performed the coimmunoprecipitation assays to show that the B55β coimmunoprecipitates with both PP2A structural (A) and catalytic (C) subunits (Figure 3D). Furthermore, in an in vitro PP2A assay using a synthetic phosphothreonine peptide RRA(pT)VA as a substrate (Chen et al., 2004), the immunoprecipitates of B55β from Dox-treated DLD1-*PPP2R2B* cells clearly displayed increased PP2A activity compared to the controls (Figure 3E), validating that *PPP2R2B* re-expression restored the loss of the associated PP2A activity in CRC cells. To confirm that dephosphorylation of p70S6K (T421/424) or Myc on *PPP2R2B* re-expression requires PP2A activity, we depleted the A subunit of PP2A complex by siRNA in DLD1-*PPP2R2B* cells and showed that this manipulation clearly prevented the dephosphorylation of Myc and p70S6K by *PPP2R2B* (Figure 3F). Together, these experiments provided evidence demonstrating a functional role of PP2A-B55β complex in modulating p70S6K and Myc phosphorylation. In addition, we have detected the p70S6K in PP2A-B55β immunoprecipitates (Figures S3A and S3B), but we were unable to detect the physical interaction between Myc with B55β. Although another PP2A subunit B56α has been previously shown to interact and dephosphorylate Myc in HEK293 cells (Arnold and Sears, 2006; Junttila et al., 2007), B55β-PP2A complex may modulate Myc phosphorylation indirectly in CRC cells.

Finally, we evaluated the functional significance of Myc and p70S6K downregulation in CRC. We found that Myc knockdown strongly suppressed DLD1 cell viability, whereas p70S6K knockdown did not yield a significant effect (Figure 3G). Moreover, *PPP2R2B* re-expression did not induce further growth inhibition when Myc was depleted in the cells (Figure 3H). Thus, this data indicate a functional contribution of Myc inhibition, to the growth inhibitory effect of B55β. This is consistent with the established role of Myc in colorectal tumorigenesis (Korinek et al., 1997; Morin et al., 1997; Sansom et al., 2007).

PPP2R2B Re-Expression Sensitizes mTORC1 Inhibitor Rapamycin

The mTOR kinase inhibitor rapamycin has a sporadic anticancer activity and its effect on mTOR downstream substrate p70S6K is often used as a surrogate marker to evaluate rapamycin response (Sawyers, 2008). The plausible connection between B55β and p70S6K signaling prompted us to investigate the possibility that *PPP2R2B* expression status may affect the cellular sensitivity to rapamycin.

We thus compared the effect of rapamycin on cell viability of DLD1-*PPP2R2B* cells in the presence or absence of Dox. The data showed that rapamycin-induced growth inhibition was much more effective when *PPP2R2B* was reexpressed after Dox treatment, as measured by either the cell viability assay for 5 days or the colony formation assay for 14 days (Figures 4A and 4B). In addition, cell cycle analysis by flow cytometry shows that Dox induction of *PPP2R2B* expression resulted in cell cycle G2 arrest, which is further markedly augmented by adding rapamycin, indicating that B55β and rapamycin synergistically induced cell cycle arrest (Figure 4C).

To verify the in vitro results in vivo, we studied the effects of rapamycin on the xenograft tumor growth in nude mice using DLD1-*PPP2R2B* with or without co-treatment with Dox. Although the rapamycin or Dox treatment alone only moderately attenuated the tumor growth, their combination gave rise to a strong tumor growth inhibition in DLD1-*PPP2R2B* cells (Figure 4D). Collectively, these results obtained from both in vitro and in vivo experiments established that the *PPP2R2B* re-expression in CRC cells led to improved therapeutic effect of rapamycin. Thus, the data suggested that epigenetic loss of *PPP2R2B* may be a molecular event affecting the sensitivity of CRC to mTOR inhibitors.

Rapamycin Induces Myc Phosphorylation and Protein Accumulation in CRC Cells, which Is Overridden by *PPP2R2B* Re-Expression

A feedback mechanism leading to PI3K activation and AKT S473 phosphorylation in mTORC2-depenent manner has been linked to rapamycin resistance in cancer (O'Reilly et al., 2006; Sarbassov et al., 2006). Indeed, rapamycin treatment of CRC cells resulted in induction of AKT S473 phosphorylation, but this phosphorylation seemed to be unaffected on *PPP2R2B* re-expression (Figure 5A). On the other hand, both p70S6K and S6 phosphorylation was effectively abolished by rapamycin treatment in both vector control and *PPP2R2B* expressing cells (Figure 5A), thus excluding the possibility that *PPP2R2B*-induced rapamycin sensitization is associated with AKT S473 or p70S6K. On the contrary, and intriguingly, we found that
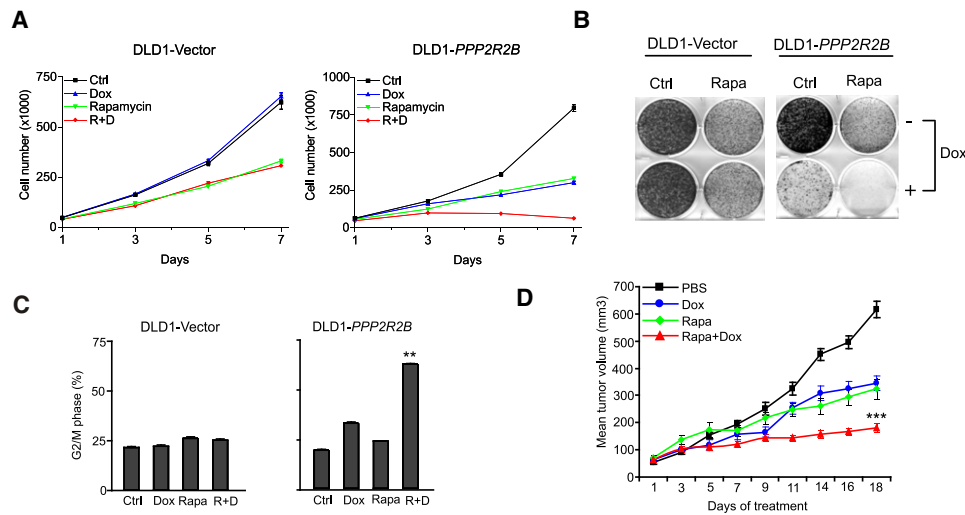
Figure 4. PPP2R2B Re-Expression in CRC Sensitizes Rapamycin Both In Vitro and In Vivo and Overrides Rapamycin-Induced Myc Phosphorylation

(A) Proliferation of DLD1-vector and DLD1-*PPP2R2B* cells treated with 10 ng/ml Dox (Dox) or 10 nM rapamycin or both (R+D) for indicated days. Error bar shows the mean ± SD of triplicates.

(B) Dense foci formation on a monolayer of DLD1-vector or DLD1-*PPP2R2B* cells treated with 10 nM rapamycin, with or without 10 ng/ml Dox treatment for 14 days.

(C) Cell cycle G2/M arrest in DLD1-vector or DLD1-*PPP2R2B* cells treated with Dox or rapamycin or both for 48 hr. Error bar shows the mean ± SD of three independent experiments.

(D) Xenograft tumor growth of DLD1-*PPP2R2B* cells in nude mice treated with Dox at 100 mg/kg, or rapamycin at 4 mg/kg or both, every other day as described in Experimental Procedures. Error bars represent ± SEM (n = 8 per group). ***p < 0.01(independent t test).

rapamycin treatment resulted in a strong induction of Myc phosphorylation and protein accumulation, which was nearly completely abolished on *PPP2R2B* re-expression (Figure 5A). This induction of Myc protein was not due to increased Myc mRNA (Figure 5B). A time course analysis indicates that the Myc response occurred as early as 4 hr, in parallel with the induction of AKT S473 phosphorylation, revealing an additional compensation event in response to mTOR inhibition (Figure 5C). We further confirmed that the rapamycin-induced Myc phosphorylation and accumulation is indeed the result of mTORC1 inhibition, as knockdown of mTOR, or raptor, an essential component of mTORC1, but not mTORC2 component rictor, resulted in a similar induction of Myc phosphorylation (Figure 5D). Given the important role of Myc in CRC tumorigenesis, this observation immediately suggests a possible mechanism underlying the *PPP2R2B*-mediated sensitization to rapamycin.

To substantiate the association of *PPP2R2B* expression with Myc response and rapamycin sensitivity, we compared the HCT116 cells with *DNMTs*-deficient HCT116 (DKO) cells in which *PPP2R2B* becomes re-expressed as a result of promoter demethylation (see Figure 1I). As in DLD1 cells, Myc phosphorylation was strongly induced by rapamycin in HCT116 cells, whereas in DKO cells, consistent with *PPP2R2B* re-expression, Myc protein was expressed in a low basal level, and did not respond to rapamycin (Figure S4A). Of note, AKT S473 phosphorylation, however, was similarly induced by rapamycin in both cell lines, regardless of *PPP2R2B* expression status (Figure S4A). Accordingly, DKO cells that displayed no Myc induction were more sensitive to rapamycin treatment as compared

to the parental HCT116 cells (Figure S4B). Taken together, the effect of B55β on Myc correlated well with the rapamycin response and support a role of B55β in inhibiting Myc phosphorylation and protein level and thus rapamycin sensitivity.

In contrast to colorectal cancer, the Oncomine database (Rhodes et al., 2004) revealed increased expression of *PPP2R2B* in several other human malignancies, including renal, liver, and ovarian cancers (Figure S4C). Real-time TaqMan assay validated the abundant expression of *PPP2R2B* in a series of cell lines derived from above tumors, including HepG2 and Hep3B cells form hepatoma; 786-O and Caki2 cells from renal carcinoma; OVCAR3, OVCAR5, and SK-OV-3 cells from ovarian carcinoma; as well as U2OS cells from osteosarcoma, as opposed to the silenced expression of *PPP2R2B* in all CRC lines (Figure S4D). Consistently, no promoter methylation was detected in *PPP2R2B*-expressing cancer cells (Figure S4E). Corresponding to the consistent silencing of *PPP2R2B* in CRC, all the CRC cell lines we have examined exhibited a marked induction of Myc phosphorylation on rapamycin treatment (Figure 5E). By contrast, none of the *PPP2R2B*-expressing cancer cell lines showed a similar Myc induction by rapamycin. Consistently, all these CRC cell lines were in general resistant to rapamycin, showing a growth inhibition of <10% after 5 days treatment with 10 nM rapamycin (Figure 5F), a concentration that results in strong growth inhibition in other cancer cell lines expressing *PPP2R2B* (Figure 5F). Of notice, rapamycin can induce AKT S473 phosphorylation in both sensitive and resistant cell lines. These results together have provided evidence to show: (1) the *PPP2R2B* silence or expression in cancer cells correlates with
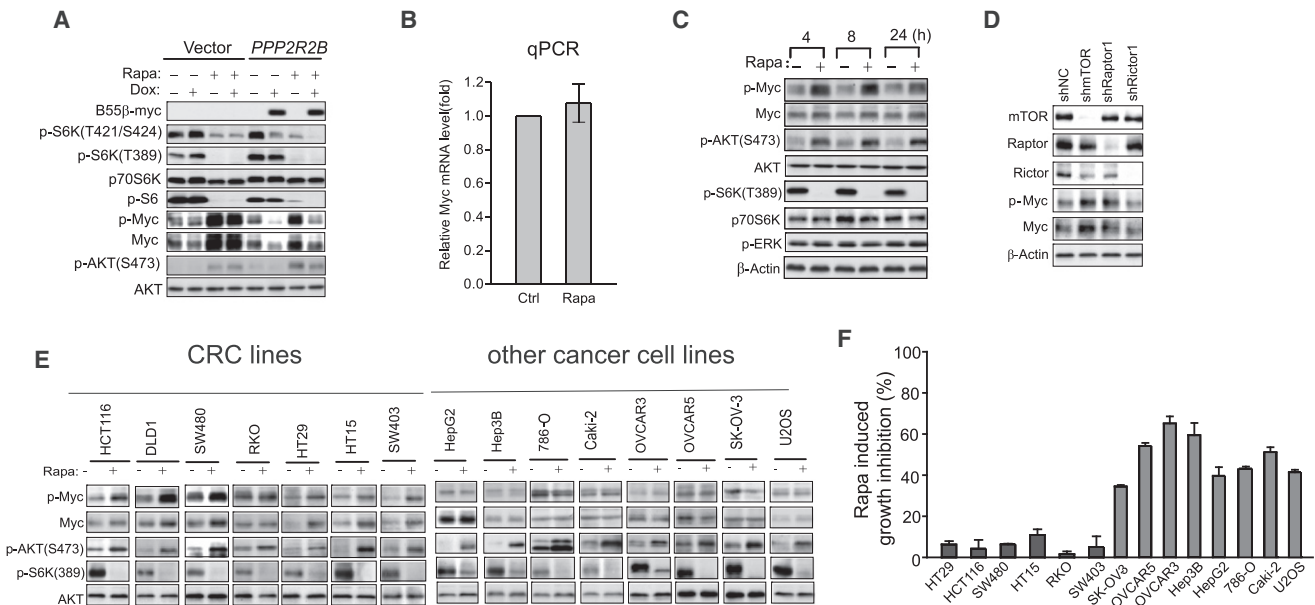
Figure 5. Rapamycin Induces Myc Phosphorylation in CRC Cell Lines

(A) DLD1-*PPP2R2B* or DLD1 vector control cells were treated with 10 nM rapamycin in the presence or absence of Dox for 48 hr. The immunoblot analysis shows that rapamycin induces Myc S62 phosphorylation, which is abrogated on *PPP2R2B* expression.

(B) TaqMan assay of Myc mRNA change in response to rapamycin treatment. Bar shows the mean ± SD of triplicates.

(C) Immunoblot analysis of indicated proteins in DLD1 cells treated with 10 nM rapamycin for the indicated times.

(D) Immunoblot analysis of Myc in DLD1 cells treated with shRNAs targeting mTOR, raptor, or rictor.

(E) Immunoblot analysis of indicated proteins in CRC and non-CRC cell lines that express *PPP2R2B*, treated with or without rapamycin.

(F) Growth inhibition induced by rapamycin in CRC cell lines and non-CRC cancer cell lines as assessed by CellTiter-Glo Luminescent Cell Viability Assay and normalized to untreated cells. Bar shows the mean ± SD of triplicates. See also Figure S4.

the sensitivity or resistance to rapamycin; and (2) this correlation is associated with, at least in part, the ability of rapamycin to induce Myc phosphorylation.

Rapamycin-Induced Myc Phosphorylation Is PDK1 Dependent but *PIK3CA*-AKT Independent

mTORC2-dependent AKT S473 phosphorylation depends on receptor tyrosine kinase (RTK) signaling on growth factor stimulation, and *PIK3CA* (encoding p110α) is required for this process (Guertin and Sabatini, 2007; Sekulic et al., 2000; Jia et al., 2008; Knight et al., 2006; Zhao et al., 2006). We found that serum starvation abolished rapamycin-induced AKT S473 phosphorylation but had no significant effect on rapamycin-induced Myc phosphorylation (Figure 6A). In addition, PIK-103, a dual *P1K3CA* and mTORC1 inhibitor (Fan et al., 2006), reduced AKT S473 phosphorylation, but enhanced Myc phosphorylation (Figure 6B).These findings suggest that rapamycin induces Myc phosphorylation through a distinct mechanism that does not depend on *P1K3CA*.

To further elucidate the upstream signals leading to rapamycin-induced Myc phosphorylation, we knocked down several major components in the PI3K and mTOR pathway. The results show that PDK1 knockdown effectively inhibited rapamycin-induced Myc phosphorylation, whereas knockdown of *PIK3CA*, *PIK3CB*, or *AKT*1 had no such an effect (Figure 6C). Further experiments with two additional PDK1 siRNAs and a PDK1 shRNA in DLD1 and SW480 cells confirmed its effect on Myc phosphorylation (Figures 6D and 6E); of note, PDK1 knockdown had no discernible

effect on AKT-S473 phosphorylation, which, however, can be clearly abolished by *PIK3CA* knockdown (Figure 6C). To substantiate this finding, we made use of a specific small molecule inhibitor of PDK1, BX912 (Feldman et al., 2005) and a specific p110α inhibitor PIK90 (Fan et al., 2006; Knight et al., 2006). Consistent with PDK1 knockdown, BX912 treatment abolished rapamycin-induced Myc phosphorylation (Figure 6F), but had no much effect on AKT S473. Conversely, PIK90 was unable to inhibit rapamycin-induced Myc phosphorylation; but effectively abolished the AKT S473 phosphorylation (Figure 6F). Taken together, these results provided convincing evidence to show that rapamycin induces a separate PDK1-dependent Myc phosphorylation, in addition to *PIK3CA*-sensitive AKT S473 phosphorylation.

Furthermore, we investigated whether ectopic expression of PDK1 can lead to Myc phosphorylation. Cotransfection of PDK1 and Myc in 293T cells resulted in a huge induction of Myc phosphorylation and protein accumulation (Figure 6G), and this induction of Myc was effectively abolished by PDK1 inhibitor BX912, but not by p110α inhibitor PIK90 (Figure 6H). Ectopic PDK1 can also induced endogenous Myc phosphorylation in immortalized mammary epithelial MCF10A and HEK-TERV cells (Figure 6I). Collectively, these results demonstrate a role of PDK1 in Myc regulation.

B55β Binds to and Inhibits PDK1 Recruitment to Cell Membrane for Activation

We next tested the possibility that B55β may directly interact with PDK1. Cotransfection of *PPP2R2B* and PDK1 plasmids in
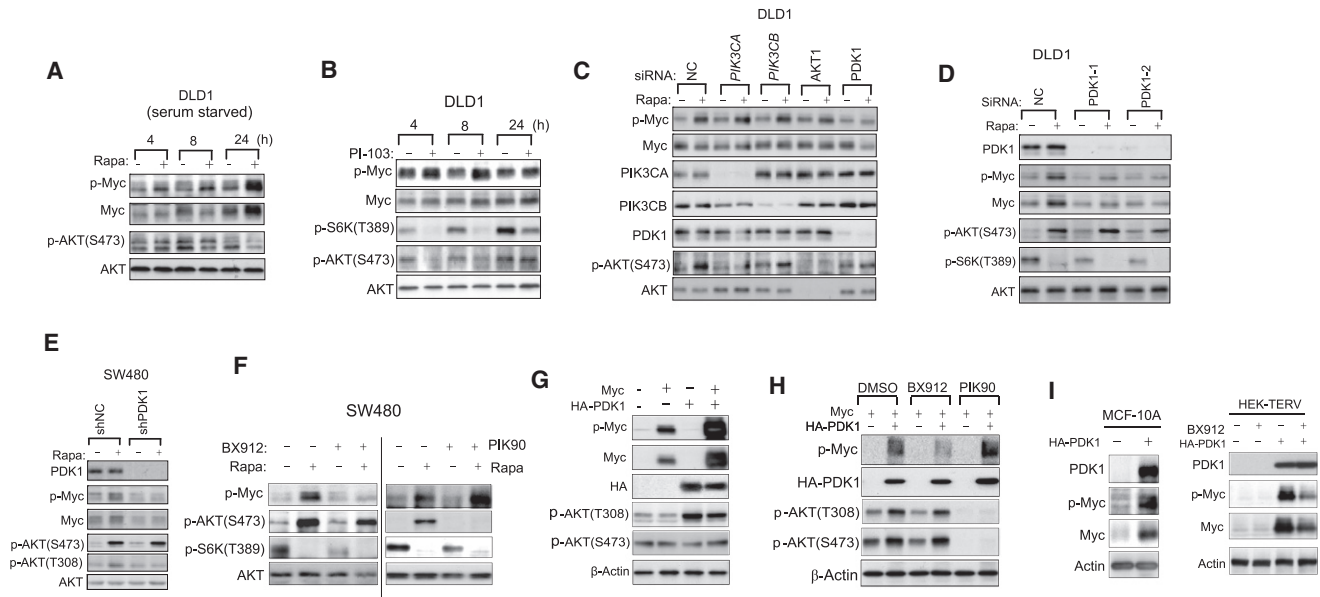
Figure 6. Rapamycin-Induced Myc Phosphorylation Requires PDK1 but not PI3K-AKT

(A) Immunoblot analysis of DLD1 cells for AKT and Myc. DLD1 cells were serum starved for 48 hr and followed by treatment with 10 nM rapamycin for the indicated times.

(B) Immunoblot analysis of DLD1 cells for AKT and Myc in response to a dual mTORC1 and P110α inhibitor PI-103 (0.5 μM) for the indicated times.

(C) Immunoblot analysis of DLD1 cells for Myc, AKT, PI3K, or PDK1. Cells were transfected with siRNAs targeting the indicated genes or a negative control siRNA for 48 hr, followed by 10 nM rapamycin treatment for 24 hr.

(D) Immunoblot analysis of PDK1, Myc and AKT in DLD1 cells transfected with two different PDK1 siRNAs or a negative control siRNA and then treated with 10 nM rapamycin for 24 hr.

(E) Immunoblot analysis of PDK1, Myc, and AKT in SW480 cells infected with a retroviral PDK1 shRNA.

(F) Immunoblot analysis of Myc, AKT, and S6K in DLD1 cells treated with PDK1 inhibitor BX912 (2.5 μM), or p110α inhibitor PIK90 (5 μM), rapamycin (10 nM) or indicated combinations for 48 hr.

(G) Immunoblot analysis of Myc in 293T cells transfected with Myc, PDK1, or both.

(H) Immunoblot analysis of Myc in 293T cells transfected with Myc, PDK1, or both, treated with or without PDK1 inhibitor BX912, or *PIK3CA* inhibitor PIK90.

(I) Immunoblot analysis of endogenous Myc in MCF10A and HEKTERV cells expressing exogenous PDK1.

293T cells showed that ectopic PDK1 coimmunoprecipitated with the B55β-Myc and vice versa (Figure 7A). This was further confirmed in DLD1-*PPP2R2B* cells in which Dox-induced B55β coimmunoprecipitated with endogenous PDK1 (Figure 7B). To show the interaction between the endogenous PDK1 and *PPP2R2B* proteins, we took the advantage of HEK-TERV and HEK-TERV-*PPP2R2B* (B55β) shRNA cells and conducted the coimmunoprecipitation experiments using PDK1 and B55 antibody, respectively. The result shows that the endogenous PDK1 clearly interacted with total B55 and this interaction was largely diminished on B55β depletion (Figure 7C). This result indicates that out of four B55 subunits B55β is a major one that interacts with PDK1. It is known that on activation PDK1 is phosphorylated and recruited from the cytosol to the plasma membrane for activation (Kikani et al., 2005). Both B55β and PDK1 are predominately located in the cytoplasm (Figures S5A and S5B), and on *PPP2R2B* re-expression, PDK1 was found to be downregulated in the plasma membrane (Figure 7D). Moreover, in serum-starved DLD1-*PPP2R2B* cells, ectopic PDK1-HA was mainly detected in the cytosol, but expressed in both cytosol and cell membrane on serum stimulation, which was abolished when cells were treated with Dox to induce *PPP2R2B* expression (Figure 7E). As a consequence of this inhibitory effect

on PDK1 membrane localization, we show that p-PKCζ(T410), a known PDK1 substrate was downregulated by *PPP2R2B* re-expression or PDK1 knockdown, although other examined PDK1 substrates did not seem to be significantly regulated by PDK1 in DLD1 cells and were thus not affected by *PPP2R2B* re-expression (Figure 7F). Taken together, the results demonstrate that B55β-PP2A complex binds to and inhibits PDK1 membrane recruitment, resulting in inhibition of its activity toward its downstream substrates. Because Myc is accumulated mainly in the nucleus in response to rapamycin (Figure S5C), the effect of cytoplasmic B55β -PDK1 on Myc is most likely to be indirect and may route through PDK1 downstream kinase substrates.

Finally, Immunohistochemistry (IHC) staining with p-PDK1 (S241) and p-PDK1-(S410) showed a clear differential staining between malignant and nonmalignant mucosal tissues. Although membrane expression of PDK-1 S241 is detected in 36.1% (35 of 97) in tumor tissues, it is only 2.7% (2 of 74) in normal cases (Figure 7F). In addition, 80.2% (77 of 96 cases) of the tumor samples exhibit intense cytoplasmic expression of PDK-1 S410, whereas it was detected mainly in the nucleus (81.9%, 59 of 72) of normal cells (Figure 7G). These findings are consistent with an active role of PDK1 toward its substrate in the
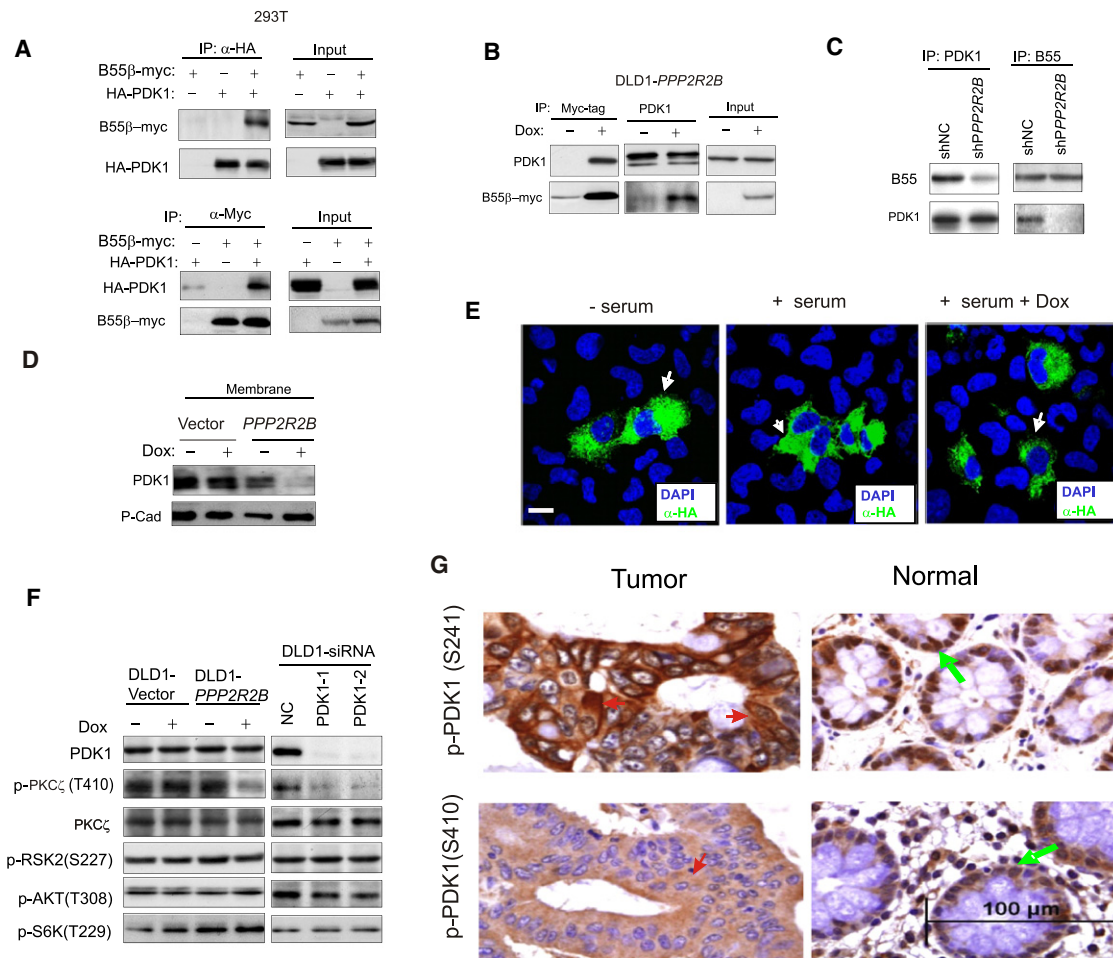
Figure 7. *PPP2R2B* Interacts with PDK1 and Inhibits Its Membrane Localization

(A) Coimmunoprecipitation assay in 293T cells transfected with B55β -Myc, PDK1-HA, or both.

(B) Coimmunoprecipitation assays in DLD1-*PPP2R2B* cells. Cells were treated with or without Dox for 24 hr and B55β-Myc or PDK1 were pulled down and subjected to immunoblot analysis.

(C) Coimmunoprecipitation assays in HEKTERV and HEKTERV-sh*PPP2R2B* cells using B55 antibody and PDK1 antibody, respectively. The endogenous interaction between PDK1 and B55β was markedly reduced in HEKTERV expressing sh*PPP2R2B*.

(D) Immunoblotting analysis of the membrane fractions on PDK1 prepared from DLD-*PPP2R2B* cells treated with or without Dox for 48 hr.

(E) Immunofluorescence for PDK1-HA in DLD1-*PPP2R2B* with or without serum and Dox treatment. Scale bar, 10 μM.

(F) Immunoblotting analysis of known PDK1 substrates on *PPP2R2B* re-expression or PDK1 knockdown in DLD1 cells.

(G) Representative images of immunohistochemical (IHC) analysis of phosphorylated PDK1 in human colon and normal mucosa. Dark brown color represents positive signal of phospho-PDK1 at S241 (upper panel) and S410 (lower panel), and blue color represents the nuclear staining. See also Figure S5.

cytoplasm/membrane, whereas its nuclear localization may restrict its function in cell proliferation (Lim et al., 2003). We thus conclude that PDK1 activity is differentially regulated in majority of colon tumors as compared to the normal tissues. Although the mutations of *PIK3CA* and *PTEN*, which occurs in 50% of CRC, contribute to the activation of PDK1, the loss of *PPP2R2B* in >90% of CRC may provide additional mechanism leading to PDK1 activation.

Inhibition of PDK1 and Myc, but Not *PIK3CA* and AKT, Sensitizes Therapeutic Response of Rapamycin

We next evaluated how the two distinct signaling pathways contribute to rapamycin resistance. PDK1 or Myc knockdown resulted in markedly increased sensitivity of rapamycin in HCT116 cells, whereas *PIK3CA* or *AKT* knockdown did not give rise to a similar effect (Figure 8A). The effect of PDK1 ablation on Myc and rapamycin sensitivity was further validated in SW480 cells expressing a retroviral PDK1 shRNA (Figure 8B). By contrast, PDK1 knockdown did not sensitize rapamycin in *PPP2R2B* expressing U2OS, Hep3B, and SKOV3 cells (Figure S6A). These results support a causal relationship between PDK1-Myc induction and rapamycin resistance in CRC cells. Moreover, the data argue for a more important role of PDK1-Myc signaling, as compared with p110α-AKT signaling, in rapamycin resistance in CRC cells.

Identification of B55β-regulated PDK1 suggests a practical approach for overcoming rapamycin resistance, which may be achieved through pharmacological inhibition of PDK1. We found
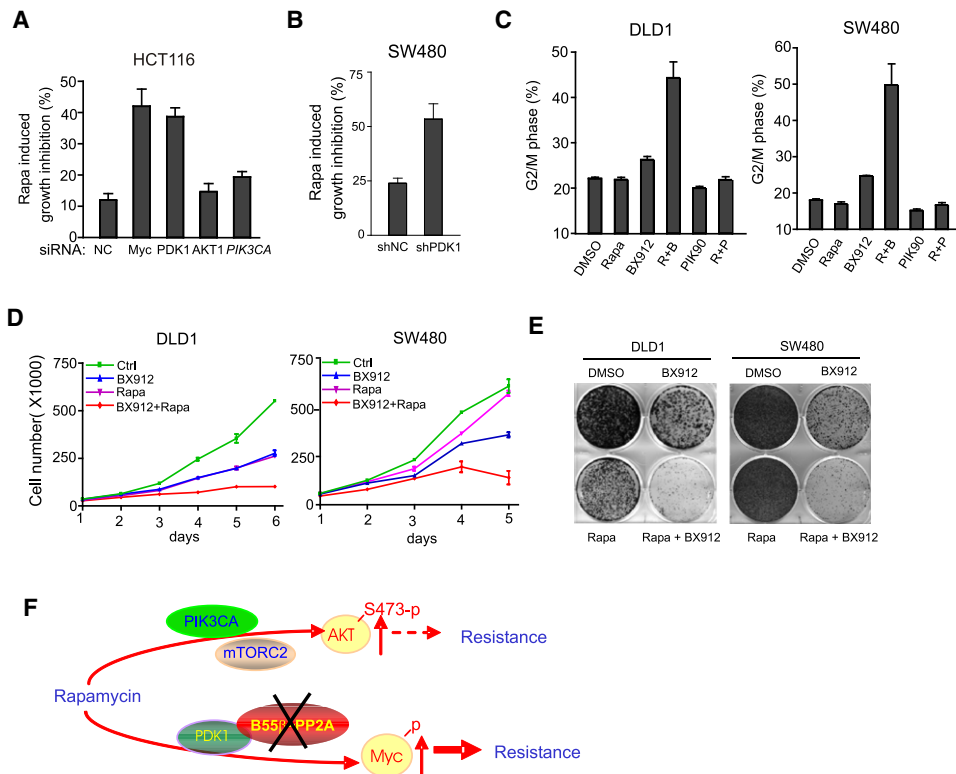
Figure 8. Inhibition of PDK1-Myc Signaling Overcomes Rapamycin Resistance
(A) HCT116 cells were transfected with siRNAs targeting *Myc*, *PDK1*, *AKT1*, or *PIK3CA* for 48 hr, and then treated with 100 nM rapamycin for 5 days. The graph bars show the rapamycin-induced growth inhibition relative to nontreated cells.
(B) Rapamycin-induced growth inhibition in SW480 cells expressing PDK1 shRNA or a negative control shRNA.
(C) G2/M phase arrest in SW480 and DLD1 cells induced by rapamycin (10 nM), BX912 (2.5 μM), PIK90 (5 μM), single or in combinations, assessed by PI staining and FACS analysis. Data are presented as mean ± SD of the percentages of cells arrested in G2/M.
(D) Cell viability of DLD1 and SW480 cells treated with BX912 (2.5 μM), rapamycin (10 nM), or both for indicated days.
(E) Dense foci formation for 14 days on a monolayer of DLD1 and SW480 cells treated as (D).
(F) A model indicating a role of B55β-regulated PDK1-Myc pathway in modulating rapamycin response. Loss of *PPP2R2B* expression in CRC results in induction of PDK1-dependent Myc phosphorylation by rapamycin, conferring rapamycin resistance. Data in (A–D) represent the mean ± SD of three independent experiments per panel. See also Figure S6.

that PDK1 shRNA or BX912, but not PIK90, induced a morphological change similar to that seen on *PPP2R2B* re-expression (Figure S6B). Moreover, BX912, but not PIK90, synergized with rapamycin to induce strong G2/M arrest in CRC cells (Figure 8C; Figure S6C), which is again remarkably reminiscent of the synergistic effect between *PP2R2B* restoration and rapamycin on G2/M induction (see earlier Figure 4C). Thus, pharmacologic inhibition of PDK1, but not p110α, has phenocopied the effect of *PPP2R2B* re-expression, further supporting the genetic interaction between B55β and PDK1. As such, we observed a synergistic loss of cell viability between BX912 and rapamycin in CRC cells in both a 5 day cell viability assay (Figure 8D) and a 2 week colony formation assay (Figure 8E). These findings support a model in which the loss of *PPP2R2B* in CRC results in activation of PDK1-dependent Myc phosphorylation in response to rapamycin treatment, leading to rapamycin resistance in a p110α-AKT independent manner (Figure 8F). Pharmacologic inhibition of PDK1 can overcome rapamycin resistance by preventing Myc phosphorylation, pointing to a potential combination strategy for CRC treatment.

DISCUSSION

We have demonstrated here that *PPP2R2B*, encoding PP2A regulatory B55β subunit, is epigenetically inactivated by DNA hypermethylation in colorectal cancer. Despite the fact that the tumor suppressor function of PP2A had been well-demonstrated in transformed model systems (Chen et al., 2004, 2005; Sablina et al., 2007; Zhao et al., 2003), PP2A subunits have been found to be mutated or deleted only in 8%–15% of human cancers. Our study now identifies that the epigenetic loss of *PPP2R2B* occurs in >90% of colorectal tumor samples. In addition to colorectal cancer, *PPP2R2B* may also be downregulated in other cancers such as bladder, brain and esophagus carcinoma, as revealed by Oncomine database. Thus, considering the low frequency of PP2A mutations among various subunits (<15%), the epigenetic mechanism leading to PP2A inactivation may play a more dominant role in human cancer like CRC.

Due to the substrate diversity of PP2A regulatory subunits, it is not surprising to see numerous oncogenic signaling pathways affected in various tissues or cellular contexts. We

hypothesize that the loss of *PPP2R2B* associated specific PP2A complex may promote the deregulation of certain onco-gene signaling pathways required for CRC cell survival and proliferation. Myc appears to be a crucial downstream target of PP2A-B55β and inactivation of Myc by PP2A-B55β is consistent with the strong growth inhibition effect of B55β on CRC cells. Although a distinct PP2A subunit B56α has been shown to associate with Myc and regulates its stability (Arnold and Sears, 2006; Junttila et al., 2007), we show that B55β-PP2A routes through PDK1 to regulate Myc. Thus, loss of *PPP2R2B* provides an additional mechanism leading to deregulation of PDK1 and Myc in CRC.

Our study reveals a previously undescribed mechanism leading to rapamycin resistance. The PDK1-Myc signaling is independent of p110α (encoded by *PIK3CA-AKT*) and may constitute an alternative feedback mechanism leading to rapamycin resistance. Although p110α and mTORC2-dependent AKT S473 phosphorylation has been suggested to be a crucial mechanism accounting for rapamycin resistance in certain contexts (O'Reilly et al., 2006; Sarbassov et al., 2006), this pathway in CRC may not be as critical as rapamycin-induced Myc phosphorylation for rapamycin resistance, as knockdown of *PIK3CA* or AKT, does not sensitize rapamycin. As such, we propose a PI3K/AKT-independent signaling module comprised of PDK1 and Myc contributing to rapamycin resistance in CRC. This notion seems to be consistent with a recent finding that AKT is often not required for proliferation of cancer cells with activated PI3K pathway (Vasudevan et al., 2009). This study widens our understanding of cancer cell growth control and rapamycin resistance and emphasizes the importance of epigenetic mechanisms in regulating oncogenic signaling and therapeutic response. However, although we demonstrate Myc as a downstream target of PDK1, PDK1 may not regulate Myc directly. It is possible that PDK1 may route through other downstream kinases to affect Myc phosphorylation. The precise feedback mechanism leading to the induction of Myc phosphorylation by rapamycin remains unclear and warrants further investigation.

Our findings may have implications for clinical application of rapamycin derivatives in human cancer. Several rapamycin analogs have been under the clinical development (Easton and Houghton, 2006; Faivre et al., 2006; Granville et al., 2006), but the therapeutic response to rapamycin is highly variable, indicating a strong need for biomarkers that are capable of predicting the therapeutic effect of rapamycin. Our data suggest that *PPP2R2B* may serve as one of the predictive markers for patient selection, whereas Myc phosphorylation can be used a surrogate marker to evaluate the drug response.

Finally, our data support PDK1 as a therapeutic target in CRC, as removal of PDK1 reduces Myc signaling and alleviates rapamycin resistance. This notion was further illustrated using a small molecule PDK1 inhibitor BX912, which is able to abolish rapamycin-induced Myc phosphorylation and thus synergizes with rapamycin in CRC. Notably, the PDK1 inhibitor as an anti-cancer agent has been shown to be effective in vitro and in vivo in cancer (Maurer et al., 2009; Peifer and Alessi, 2008) and is currently under clinical development. Therefore, uncovering a PDK1-Myc pathway allows us to propose that targeting of PDK1 may become a useful treatment strategy for Myc-driven tumors.

EXPERIMENTAL PROCEDURES

Clinical Samples, Cell Lines, and Drugs

Human tissue samples were obtained from Singapore Tissue Network and National University of Singapore using protocols approved by the Institutional Review Board of the National University of Singapore (NUS-IRB); informed consent was obtained from each individual who provided the tissues. The cancer cell lines used in this study were purchased from the American Type Culture Collection (Manassas, VA). HCT116 cells with genetic disruption of *DNMT1* and *DNMT3B* (HCT116 DKO) were kindly provided by Dr. Bert Vogelstein (Johns Hopkins University, MD).HEK-TERV cells were a generous gift from Dr. W.C. Hahn at Dana-Farber Cancer Institute. 5-AzaC and Doxycycline were purchased from Sigma. Rapamycin and PI-103 were purchased from Alexis (San Diego, CA). PDK1 inhibitor BX912 and the *PIK3CA* inhibitor PIK90 were obtained from Axon Medchem (Groningen, The Netherlands).

Plasmids and Stable Cell Lines

Information for *PPP2R2B* plasmid and stable cell lines construct are provided in Supplemental Experimental Procedures.

Illuminar Gene Expression, Semiquantitative RT-PCR, and TaqMan Assay

Illuminar gene expression data of human CRC and matched normal controls have been described previously (Jiang et al., 2008) and can be found at the Gene Expression Omnibus public database (accession number GSE10972). Details for RT-PCR and TaqMan assay are provided in Supplemental Experimental Procedures.

DNA Methylation Analysis

Bisulfite modification of DNA was carried out by using the EZ DNA methylation-Gold kit (ZYMO Research) according the manufacture's instructions. The CpG island DNA methylation status was determined by methylation-specific PCR (MSP) and bisulfite genomic sequencing (BGS) as previously described (Jiang et al., 2008). Details are provided in Supplemental Experimental Procedures.

Antibodies

The following antibodies were used: Myc, p70-S6K, p-p70S6K(T421/S424), p-p70S6K(T389), p-p70S6K(S371), p-AKT (S473), p-AKT (T308), AKT, p-RSK2 (S227), p-PKCζ(T410), PKCζ, mTOR, Raptor, Rictor, PDK1(S241), S6, p-S6 (S235/236), p-MEK1/2(S217/221), p-ERK1/2(T202/Y204), p-p38MAPK(T180/Y182), PP2A A Subunit(81G5), p110α, and p110β (Cell Signaling Technology). p-PDK1(S410) (Abcam), β-catenin and PDK1 (BD Biosciences), anti-PP2A B subunit (B55) (Upstate Biotechnology), p-Myc(S62) (BioAcademia), HA (SC-805) and β-Actin (Santa Cruz Biotech), Myc (9E10) (Sigma-Aldrich), and p-S6K(T229) (R&D Systems).

RNA Interference

The SMARTpool siRNA targeting *PPP2R2B* and the nontargeting control were purchased from Dharmacon (Lafayette, CO). A separate *PPP2R2B* siRNA targeting the following sequence: 5′-GCUUACUUUCUUCUGUCUA-3′ was obtained from Sigma-Proligo. Cells were transfected with 100 nM final concentration of siRNA duplexes using Lipofectamine RNAiMAX (Invitrogen) following the manufacturer's instructions. To generate *PPP2R2B* shRNA stable cell, the targeted sequence (GCUUACUUUCUUCUGUCUA-3′) was cloned into the pSIREN-RetroQ-ZsGreen retroviral expression vector (BD Bioscience). The pSIREN-RetroQ-Neg vector was used as negative control shRN (BD Bioscience), and cells were sorted with GFP for further analysis. Details for other siRNAs and shRNA used in this study are provided in Supplemental Experimental Procedures.

Coimmunoprecipitation

For immunoprecipitation analysis, 293T cells were transiently transfected with HA-PDK1 and *PPP2R2B*-Myc by using Fugen HD (Roche). At 48 hr posttranfection, the cells were lysed and immunoprecipitated with antibodies for HA-tag (SC-805, Santa, Cruz) and Myc-tag (9E10, Roche). To study direct interaction between B55β-Myc and endogenous PDK1, DLD1-*PPP2R2B* cells

were treated with Dox for 24 hr and cells were lysed and immunoprecipitated with anti-PDK1 and anti-Myc-tag.

Tumor Xenografts
All animal studies were conducted in compliance with animal protocols approved by the ASTAR-Biopolis Institutional Animal Care and Use Committee (IACUC) of Singapore. Details are provided in Supplemental Experimental Procedures.

Soft Agar and Cell Proliferation Assay
Methods are described in Supplemental Experimental Procedures.

Confocal and Immunohistochemistry
Confocal and immunohistochemistry for cell line and human samples were carried out as described in Supplemental Experimental Procedures.

In Vitro Phosphatase Assay
For phosphatase assays, DLD1-*PPP2R2B* or DLD1 control cells were suspended in lysis buffer (50 mM Tris-HCl, pH 7.4, 7.5% Glycerol, 1 mM EDTA, 150 mM NaCl, 0.5% NP-40, 1 mM Na3VO4, Complete Protease Inhibitor), cleared from debris by centrifugation, incubated with c-Myc (9E10, Roche) followed by incubation with Anti-Mouse IgG Beads (Roche). The beads were resuspended in PP2A phosphatase reaction buffer and analyzed for PP2A activity using Serine/Threonine Phosphatase Assay kit (Upstate) according to the manufacturer's specifications. Fluorescence was measured using a fluorescence microplate reader (Sunrise, Tecan).

Statistical Analysis
All values from in vitro assays are expressed as mean ± SD or SEM of at least three independent experiments or replicates. P values were calculated with the two-tailed Student's t test. A p value <-0.05 is considered statistically significant.

SUPPLEMENTAL INFORMATION

Supplemental Information includes Supplemental Experimental Procedures, Supplemental References, six figures, and two tables and can be found with this article online at doi:10.1016/j.ccr.2010.10.021.

REFERENCES

Andrabi, S., Gjoerup, O.V., Kean, J.A., Roberts, T.M., and Schaffhausen, B. (2007). Protein phosphatase 2A regulates life and death decisions via Akt in a context-dependent manner. Proc. Natl. Acad. Sci. USA *104*, 19011–19016.

Arnold, H.K., and Sears, R.C. (2006). Protein phosphatase 2A regulatory subunit B56alpha associates with c-myc and negatively regulates c-myc accumulation. Mol. Cell. Biol. *26*, 2832–2844.

Arnold, H.K., and Sears, R.C. (2008). A tumor suppressor role for PP2A-B56alpha through negative regulation of c-Myc and other key oncoproteins. Cancer Metastasis Rev. *27*, 147–158.

Calin, G.A., di Iasio, M.G., Caprini, E., Vorechovsky, I., Natali, P.G., Sozzi, G., Croce, C.M., Barbanti-Brodano, G., Russo, G., and Negrini, M. (2000). Low frequency of alterations of the alpha (PPP2R1A) and beta (PPP2R1B) isoforms of the subunit A of the serine-threonine phosphatase 2A in human neoplasms. Oncogene *19*, 1191–1195.

Chen, W., Possemato, R., Campbell, K.T., Plattner, C.A., Pallas, D.C., and Hahn, W.C. (2004). Identification of specific PP2A complexes involved in human cell transformation. Cancer Cell *5*, 127–136.

Chen, W., Arroyo, J.D., Timmons, J.C., Possemato, R., and Hahn, W.C. (2005). Cancer-associated PP2A Alpha subunits induce functional haploinsufficiency and tumorigenicity. Cancer Res. *65*, 8183–8192.

Easton, J.B., and Houghton, P.J. (2006). mTOR and cancer therapy. Oncogene *25*, 6436–6446.

Eichhorn, P.J., Creyghton, M.P., and Bernards, R. (2009). Protein phosphatase 2A regulatory subunits and cancer. Biochim. Biophys. Acta *1795*, 1–15.

Faivre, S., Kroemer, G., and Raymond, E. (2006). Current development of mTOR inhibitors as anticancer agents. Nat. Rev. Drug Discov. *5*, 671–688.

Fan, Q.W., Knight, Z.A., Goldenberg, D.D., Yu, W., Mostov, K.E., Stokoe, D., Shokat, K.M., and Weiss, W.A. (2006). A dual PI3 kinase/mTOR inhibitor reveals emergent efficacy in glioma. Cancer Cell *9*, 341–349.

Feldman, R.I., Wu, J.M., Polokoff, M.A., Kochanny, M.J., Dinter, H., Zhu, D., Biroc, S.L., Alicke, B., Bryant, J., Yuan, S., et al. (2005). Novel small molecule inhibitors of 3-phosphoinositide-dependent kinase-1. J. Biol. Chem. *280*, 19867–19874.

Granville, C.A., Memmott, R.M., Gills, J.J., and Dennis, P.A. (2006). Handicapping the race to develop inhibitors of the phosphoinositide 3-kinase/Akt/mammalian target of rapamycin pathway. Clin. Cancer Res. *12*, 679–689.

Guertin, D.A., and Sabatini, D.M. (2007). Defining the role of mTOR in cancer. Cancer Cell *12*, 9–22.

Hahn, W.C., Dessain, S.K., Brooks, M.W., King, J.E., Elenbaas, B., Sabatini, D.M., DeCaprio, J.A., and Weinberg, R.A. (2002). Enumeration of the simian virus 40 early region elements necessary for human cell transformation. Mol. Cell. Biol. *22*, 2111–2123.

Hudes, G., Carducci, M., Tomczak, P., Dutcher, J., Figlin, R., Kapoor, A., Staroslawska, E., Sosman, J., McDermott, D., Bodrogi, I., et al. (2007). Temsirolimus, interferon alfa, or both for advanced renal-cell carcinoma. N. Engl. J. Med. *356*, 2271–2281.

Janssens, V., and Goris, J. (2001). Protein phosphatase 2A: a highly regulated family of serine/threonine phosphatases implicated in cell growth and signalling. Biochem. J. *353*, 417–439.

Jia, S., Liu, Z., Zhang, S., Liu, P., Zhang, L., Lee, S.H., Zhang, J., Signoretti, S., Loda, M., Roberts, T.M., et al. (2008). Essential roles of PI(3)K-p110beta in cell growth, metabolism and tumorigenesis. Nature *454*, 776–779.

Jiang, X., Tan, J., Li, J., Kivimae, S., Yang, X., Zhuang, L., Lee, P.L., Chan, M.T., Stanton, L.W., Liu, E.T., et al. (2008). DACT3 is an epigenetic regulator of Wnt/beta-catenin signaling in colorectal cancer and is a therapeutic target of histone modifications. Cancer Cell *13*, 529–541.

Junttila, M.R., Puustinen, P., Niemela, M., Ahola, R., Arnold, H., Bottzauw, T., Ala-aho, R., Nielsen, C., Ivaska, J., Taya, Y., et al. (2007). CIP2A inhibits PP2A in human malignancies. Cell *130*, 51–62.

Kikani, C.K., Dong, L.Q., and Liu, F. (2005). "New"-clear functions of PDK1: beyond a master kinase in the cytosol? J. Cell. Biochem. *96*, 1157–1162.

Knight, Z.A., Gonzalez, B., Feldman, M.E., Zunder, E.R., Goldenberg, D.D., Williams, O., Loewith, R., Stokoe, D., Balla, A., Toth, B., et al. (2006). A pharmacological map of the PI3-K family defines a role for p110alpha in insulin signaling. Cell *125*, 733–747.

Korinek, V., Barker, N., Morin, P.J., van Wichen, D., de Weger, R., Kinzler, K.W., Vogelstein, B., and Clevers, H. (1997). Constitutive transcriptional activation by a beta-catenin-Tcf complex in APC−/− colon carcinoma. Science *275*, 1784–1787.

Kuo, Y.C., Huang, K.Y., Yang, C.H., Yang, Y.S., Lee, W.Y., and Chiang, C.W. (2008). Regulation of phosphorylation of Thr-308 of Akt, cell proliferation, and survival by the B55alpha regulatory subunit targeting of the protein phosphatase 2A holoenzyme to Akt. J. Biol. Chem. *283*, 1882–1892.

Lim, M.A., Kikani, C.K., Wick, M.J., and Dong, L.Q. (2003). Nuclear translocation of 3′-phosphoinositide-dependent protein kinase 1 (PDK-1): a potential regulatory mechanism for PDK-1 function. Proc. Natl. Acad. Sci. USA *100*, 14006–14011.

Mao, J.H., Kim, I.J., Wu, D., Climent, J., Kang, H.C., DelRosario, R., and Balmain, A. (2008). FBXW7 targets mTOR for degradation and cooperates with PTEN in tumor suppression. Science *321*, 1499–1502.

Maurer, M., Su, T., Saal, L.H., Koujak, S., Hopkins, B.D., Barkley, C.R., Wu, J., Nandula, S., Dutta, B., Xie, Y., et al. (2009). 3-Phosphoinositide-dependent kinase 1 potentiates upstream lesions on the phosphatidylinositol 3-kinase pathway in breast carcinoma. Cancer Res. *69*, 6299–6306.

Morin, P.J., Sparks, A.B., Korinek, V., Barker, N., Clevers, H., Vogelstein, B., and Kinzler, K.W. (1997). Activation of beta-catenin-Tcf signaling in colorectal cancer by mutations in beta-catenin or APC. Science *275*, 1787–1790.

O'Reilly, K.E., Rojo, F., She, Q.B., Solit, D., Mills, G.B., Smith, D., Lane, H., Hofmann, F., Hicklin, D.J., Ludwig, D.L., et al. (2006). mTOR inhibition induces upstream receptor tyrosine kinase signaling and activates Akt. Cancer Res. *66*, 1500–1508.

Padmanabhan, S., Mukhopadhyay, A., Narasimhan, S.D., Tesz, G., Czech, M.P., and Tissenbaum, H.A. (2009). A PP2A regulatory subunit regulates C. elegans insulin/IGF-1 signaling by modulating AKT-1 phosphorylation. Cell *136*, 939–951.

Peifer, C., and Alessi, D.R. (2008). Small-molecule inhibitors of PDK1. ChemMedChem *3*, 1810–1838.

Peterson, R.T., Desai, B.N., Hardwick, J.S., and Schreiber, S.L. (1999). Protein phosphatase 2A interacts with the 70-kDa S6 kinase and is activated by inhibition of FKBP12-rapamycinassociated protein. Proc. Natl. Acad. Sci. USA *96*, 4438–4442.

Rangarajan, A., Hong, S.J., Gifford, A., and Weinberg, R.A. (2004). Species- and cell type-specific requirements for cellular transformation. Cancer Cell *6*, 171–183.

Rhodes, D.R., Yu, J., Shanker, K., Deshpande, N., Varambally, R., Ghosh, D., Barrette, T., Pandey, A., and Chinnaiyan, A.M. (2004). ONCOMINE: a cancer microarray database and integrated data-mining platform. Neoplasia *6*, 1–6.

Ruediger, R., Pham, H.T., and Walter, G. (2001). Alterations in protein phosphatase 2A subunit interaction in human carcinomas of the lung and colon with mutations in the A beta subunit gene. Oncogene *20*, 1892–1899.

Sabatini, D.M. (2006). mTOR and cancer: insights into a complex relationship. Nat. Rev. Cancer *6*, 729–734.

Sablina, A.A., Chen, W., Arroyo, J.D., Corral, L., Hector, M., Bulmer, S.E., DeCaprio, J.A., and Hahn, W.C. (2007). The tumor suppressor PP2A Abeta regulates the RalA GTPase. Cell *129*, 969–982.

Sansom, O.J., Meniel, V.S., Muncan, V., Phesse, T.J., Wilkins, J.A., Reed, K.R., Vass, J.K., Athineos, D., Clevers, H., and Clarke, A.R. (2007). Myc deletion rescues Apc deficiency in the small intestine. Nature *446*, 676–679.

Sarbassov, D.D., Ali, S.M., Sengupta, S., Sheen, J.H., Hsu, P.P., Bagley, A.F., Markhard, A.L., and Sabatini, D.M. (2006). Prolonged rapamycin treatment inhibits mTORC2 assembly and Akt/PKB. Mol. Cell *22*, 159–168.

Sawyers, C.L. (2008). The cancer biomarker problem. Nature *452*, 548–552.

Scott, K.L., Kabbarah, O., Liang, M.C., Ivanova, E., Anagnostou, V., Wu, J., Dhakal, S., Wu, M., Chen, S., Feinberg, T., et al. (2009). GOLPH3 modulates mTOR signalling and rapamycin sensitivity in cancer. Nature *459*, 1085–1090.

Seeling, J.M., Miller, J.R., Gil, R., Moon, R.T., White, R., and Virshup, D.M. (1999). Regulation of beta-catenin signaling by the B56 subunit of protein phosphatase 2A. Science *283*, 2089–2091.

Sekulic, A., Hudson, C.C., Homme, J.L., Yin, P., Otterness, D.M., Karnitz, L.M., and Abraham, R.T. (2000). A direct linkage between the phosphoinositide 3-kinase-AKT signaling pathway and the mammalian target of rapamycin in mitogen-stimulated and transformed cells. Cancer Res. *60*, 3504–3513.

Sontag, E., Fedorov, S., Kamibayashi, C., Robbins, D., Cobb, M., and Mumby, M. (1993). The interaction of SV40 small tumor antigen with protein phosphatase 2A stimulates the map kinase pathway and induces cell proliferation. Cell *75*, 887–897.

Su, Y., Fu, C., Ishikawa, S., Stella, A., Kojima, M., Shitoh, K., Schreiber, E.M., Day, B.W., and Liu, B. (2008). APC is essential for targeting phosphorylated beta-catenin to the SCFbeta-TrCP ubiquitin ligase. Mol. Cell *32*, 652–661.

Takagi, Y., Futamura, M., Yamaguchi, K., Aoki, S., Takahashi, T., and Saji, S. (2000). Alterations of the PPP2R1B gene located at 11q23 in human colorectal cancers. Gut *47*, 268–271.

Tamaki, M., Goi, T., Hirono, Y., Katayama, K., and Yamaguchi, A. (2004). PPP2R1B gene alterations inhibit interaction of PP2A-Abeta and PP2A-C proteins in colorectal cancers. Oncol. Rep. *11*, 655–659.

Thomas, G.V., Tran, C., Mellinghoff, I.K., Welsbie, D.S., Chan, E., Fueger, B., Czernin, J., and Sawyers, C.L. (2006). Hypoxia-inducible factor determines sensitivity to inhibitors of mTOR in kidney cancer. Nat. Med. *12*, 122–127.

Vasudevan, K.M., Barbie, D.A., Davies, M.A., Rabinovsky, R., McNear, C.J., Kim, J.J., Hennessy, B.T., Tseng, H., Pochanard, P., Kim, S.Y., et al. (2009). AKT-independent signaling downstream of oncogenic PIK3CA mutations in human cancer. Cancer Cell *16*, 21–32.

Virshup, D.M., and Shenolikar, S. (2009). From promiscuity to precision: protein phosphatases get a makeover. Mol. Cell *33*, 537–545.

Wang, S.S., Esplin, E.D., Li, J.L., Huang, L., Gazdar, A., Minna, J., and Evans, G.A. (1998). Alterations of the PPP2R1B gene in human lung and colorectal cancer. Science *282*, 284–287.

Westermarck, J., and Hahn, W.C. (2008). Multiple pathways regulated by the tumor suppressor PP2A in transformation. Trends Mol. Med. *14*, 152–160.

Yeh, E., Cunningham, M., Arnold, H., Chasse, D., Monteith, T., Ivaldi, G., Hahn, W.C., Stukenberg, P.T., Shenolikar, S., Uchida, T., et al. (2004). A signalling pathway controlling c-Myc degradation that impacts oncogenic transformation of human cells. Nat. Cell Biol. *6*, 308–318.

Zhao, J.J., Gjoerup, O.V., Subramanian, R.R., Cheng, Y., Chen, W., Roberts, T.M., and Hahn, W.C. (2003). Human mammary epithelial cell transformation through the activation of phosphatidylinositol 3-kinase. Cancer Cell *3*, 483–495.

Zhao, J.J., Cheng, H., Jia, S., Wang, L., Gjoerup, O.V., Mikami, A., and Roberts, T.M. (2006). The p110alpha isoform of PI3K is essential for proper growth factor signaling and oncogenic transformation. Proc. Natl. Acad. Sci. USA *103*, 16296–16300.